Nonlinear Peltier effect and thermoconductance in nanowires

E. N. Bogachek, A. G. Scherbakov, and Uzi Landman
School of Physics, Georgia Institute of Technology, Atlanta, Georgia 30332-0430
(Received 16 July 1998; revised manuscript received 10 May 1999)

A theoretical analysis of thermal transport in nanowires, in field-free conditions and under influence of applied magnetic fields, is presented. It is shown that in the nonlinear regime (finite applied voltage) new peaks in the Peltier coefficient appear leading to violation of Onsager's relation between the Peltier and thermopower coefficients. Oscillations of the Peltier coefficient in a magnetic field are demonstrated. The thermoconductance has a steplike quantized structure similar to the electroconductance and it exhibits deviations from the Wiedemann-Franz law. The strong dependence of the thermoconductance on the applied magnetic field leads to the possibility of magnetic blockade of thermal transport in wires with a small number of conducting channels. Possible control of thermal transport in nanowires through external parameters, that is applied through finite voltages and magnetic fields, is discussed. [S0163-1829(99)04140-5]

I. INTRODUCTION

Electric and heat transport processes between bulk reservoirs connected via a system of reduced size (microconstriction) have been the subject of numerous studies for a rather long time.[1(a)–1(c)] In recent years research pertaining to such phenomena focused particularly on ballistic transport through two-[1(b)] and three[1(c)]-dimensional (2D and 3D, respectively) constrictions (referred to also as point contacts or wires) with a transverse size (cross-sectional radius, a_o, in the case of a 3D wire) comparable to the Fermi wavelength (λ_F) of the electrons. In such cases the transport is of quantum nature, unlike the case of classical point contacts with $k_F a_o \gg 1$ (that is, in the Sharvin limit[2]), portraying the discrete character of the electronic transport modes (transverse subbands, or conducting channels) which develop in the wire due to its reduced size. The quantum nature of transport phenomena in such wires is exhibited by a step-wise quantization of the electric conductance[1(b),1(c)] (varying as a function of a gate voltage, or equivalently the width of the constriction, in steps of the conductance quantum, $2e^2/h$, or multiples thereof), as well as by quantization of the thermal conductance and a consequent peaklike (oscillatory) variation of the thermopower and Peltier coefficient (the later related to the generation of a heat current driven by an applied voltage between the connected reservoirs under isothermal conditions).[1(d),3,4] These phenomena, as well as magnetotransport processes in such 3D quantum[1(d)] wires, have been investigated mostly in the linear-response regime; for theoretical studies of finite-voltage (i.e., nonlinear) effects on electric and/or magnetoconductance in 2D and 3D quantum constrictions, see Ref. 5 and Refs. 6 and 7, respectively, and 7, respectively, and for a most recent discussion of nonlinearities in thermal transport through 2D quantum point contacts see Ref. 8.

In this paper, we focus on thermal transport properties of 3D quantum nanowires through comparative theoretical analysis of the thermal conductance and Peltier coefficients in the linear and nonlinear regimes. One of our findings pertains to significant finite-voltage effects on the behavior of the Peltier coefficient as a function of $k_F a_o$; that is, we find marked variations in the peak structure of the Peltier coefficient (including the development of new peaks) from it's linear response dependence on the Fermi energy and/or the quantum wire's lateral sizes, implying violation of Onsager's symmetry relations between the kinetic coefficients. Additionally, we find that as in the case of 2D quantum point contacts[3,4] the Wiedemann-Franz (WF) law, relating the thermal and electric conductances, which holds in classical point contacts,[9] is violated in 3D quantum wires due to the strong-energy dependence of the transmission probabilities of the conducting electrons through the wire; in this context we also demonstrate here restoration of the WF law when the energy level quantization effects are less effective, that is for short quantum wires where tunneling contributions to the transmission probabilities become significant, and/or at sufficiently low temperatures when the Fermi distribution is sharpened. Furthermore, we investigate the influence of magnetic fields on thermal transport in 3D quantum wires, and demonstrate that it may be controlled by external magnetic fields as well as by applied finite voltages.

In the following section, we introduce first the basic expressions for the electric and entropy currents in wires and review the definitions of the various transport coefficients in the context of classical point contacts where derivations of analytical expressions are possible (Sec. II). Analysis of the transport coefficients for quantum wires is given in Sec. III, and we summarize our results in Sec. IV.

II. TRANSPORT AND CLASSICAL POINT CONTACTS

We consider ballistic electric and thermal transport through a three-dimensional (3D) nanowire connecting two bulk reservoirs. A bias voltage V is applied between the reservoirs which are kept at different temperatures T_1 and T_2. Due to the existence of electrons with different temperatures in the wire thermal equilibrium cannot be established.

Thermal transport through a nanowire may be described in the entropy current formalism[9] modified in Ref. 10 for the Landauer scheme.[11] In this description the electric current I, and the entropy flow I_s,[12] are expressed in terms of the equilibrium Fermi functions f_o, of the bulk reservoirs, and have the forms (we assume the wire to be symmetric about the middle[7])

$$I=\frac{2e}{h}\int dE\left[f_o\left(\frac{E-eV/2-\mu_1}{k_BT_1}\right)-f_o\left(\frac{E+eV/2-\mu_2}{k_BT_2}\right)\right]\times\sum T_{mn;m'n'}(E), \quad (1)$$

and

$$I_s=\frac{2k_B}{h}\int dE\left[v_o\left(\frac{E-eV/2-\mu_1}{k_BT_1}\right)-v_o\left(\frac{E+eV/2-\mu_2}{k_BT_2}\right)\right]\times\sum T_{mn;m'n'}(E). \quad (2)$$

Here, the chemical potentials $\mu_i=\mu(T_i)$, $i=1$ or 2, are determined by the temperatures of the reservoirs T_i (for the case of an isotropic and quadratic dispersion law for the electrons, $\mu\simeq\varepsilon_F-(\pi k_BT)^2/12\varepsilon_F$, where ε_F is the Fermi energy and k_B is the Boltzmann constant), $T_{mn;m'n'}$ is the transmission probability for the incident mn channel, and the function v_o in Eq. (2) is the entropy density

$$v_o(x)=f_o(x)\ln f_o(x)+[1-f_o(x)]\ln[1-f_o(x)]. \quad (3)$$

The sums in Eqs. (1) and (2) run over all incident and transmitted channels.

Classical point contacts

While the focus of our study is on transport phenomena in quantum wires ($k_Fa_o\sim1$), we review first the case of large, classical, point contacts (of the Sharvin type,[2] with $k_Fa_o\gg1$) where it is possible to derive analytical expressions for the pertinent transport properties (this also allows us to conveniently introduce the various transport coefficients that we discuss for quantum constrictions in the following section). For such systems, the sums in Eqs. (1) and (2) may be approximated (assuming unit transmission probabilities) by $(ka_o)^2/4$, and for $k_BT\ll\varepsilon_F$ we obtain the following transport expressions for the electric and entropy currents[9] (compare with the corresponding equations for the electric and heat current densities in homogeneous systems[13])

$$I=-GV^*+K(T_2^2-T_1^2), \quad (4)$$

$$I_s=-K(T_1+T_2)V^*+L_oG(T_2-T_1). \quad (5)$$

Here, $V^*=V+(\mu_1-\mu_2)/e$ is the difference between the electrochemical potentials, $G=(2e^2/h)(k_Fa_o)^2/4$ is the electrical conductance of the classical 3D contact (Sharvin's conductance[2]), $K=k_B^2\pi em^*a_o^2/(12\hbar^3)$ is the thermoelectric coefficient with m^* being the electronic effective mass, and $L_0=\pi^2k_B^2/(3e^2)$ is the Lorentz number. The fact that the expressions for I and I_s involve the same thermoelectric coefficient K follows from the Onsager principle. Note that relations (4) and (5) were obtained here beyond the standard formulation of nonequilibrium thermodynamics, since the difference T_2-T_1 was not assumed to be small.

In practice determination of the various transport coefficients in Eqs. (4) and (5) requires certain arrangements of the apparatus.[13] For example to measure the electrical conductance G, the apparatus is arranged such that the specimen (here the nanowire) and reservoirs are at isothermal conditions (i.e., $T_1=T_2=T$) while a voltage difference V (or equivalently an electric field) is applied. Measurement of the electric current I allows then a determination of G.

A temperature difference $\Delta T=T_2-T_1$ between the reservoirs induces heat flow Q, through the wire. In the linear regime (with respect to ΔT), the heat flow is related to the entropy current as $Q=TI_s$. To measure the thermoconductance G_T, the system is electrically insulated, thus preventing the flow of electric current through the wire (i.e., $I=0$), and

$$G_T=\lim_{\Delta T\to0}\left(\frac{Q}{\Delta T}\right)\Bigg|_{I=0}. \quad (6)$$

Under these conditions one obtains from Eq. 4 (with $I=0$) and Eq. 5 (Ref. 9)

$$G_T=L_0\left(1-\frac{4T^2K^2}{L_0G^2}\right)TG, \quad (7)$$

where $T\equiv(T_1+T_2)/2$. To order $(k_BT/\varepsilon_F)^2$ the correction due to the second term in the bracket on the right-hand side of Eq. (7) may be neglected[13] (certainly for metals) and $G_T=L_0TG$, a relation known as the Wiedemann-Franz law.[13]

From Eq. (4) with $I=0$ and $T_2\neq T_1$ one observes the generation of a thermopower in the point contact, $\varepsilon_T\equiv V^*=K(T_2^2-T_1^2)/G$, given by

$$\varepsilon_T=\frac{\pi^2k_B^2}{6e\varepsilon_F}(T_2^2-T_1^2). \quad (8)$$

The (absolute) thermopower coefficients (the Seebeck coefficient) is defined as

$$S=\lim_{\Delta T\to0}\left(\frac{\varepsilon_T}{\Delta T}\right)\Bigg|_{I=0}, \quad (9)$$

yielding for the classical point contact (in the linear regime with respect to ΔT) (Ref. 9)

$$S=\frac{\pi^2k_B^2T}{3e\varepsilon_F}. \quad (10)$$

An additional thermoelectric phenomena that we mention here is the Peltier effect, which describes the generation of a thermal current, associated with an electric current driven in a circuit under isothermal conditions (i.e., $T_1=T_2$) by an external voltage V. The Peltier coefficient

$$\Pi=\lim_{\Delta I\to0}\left(\frac{TI_s}{\Delta I}\right)\Bigg|_{T_2=T_1=T}, \quad (11)$$

is generally related[9] to the absolute thermal power coefficient S as $\Pi=ST$ (this relation can be easily verified using Eqs. (4) and (5), with the corresponding expressions for G and K, in the above definition of Π).

III. QUANTUM WIRES

To evaluate the transport coefficients for 3D quantum nanowires (i.e., when the Fermi wavelength is of the order of the lateral size of the wire) we start from Eqs. (1) and (2) for the electric and entropy currents, in conjunction with the definitions of the various coefficients given in the previous section. To this aim we will model the nanowire as a constriction whose cross sections perpendicular to the wire's

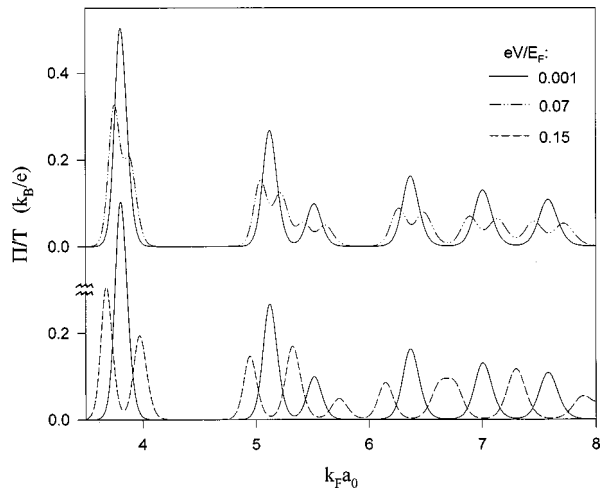

FIG. 1. The Peltier coefficient (Π, in units of k_BT/e) of a 3D wire plotted vs. the dimensionless parameter k_Fa_0, for $H=0$. $k_BT/\varepsilon_F=0.01$, $R/a_0=50$. The different curves correspond to the three marked values of the applied voltage (V in units of ε_F/e). In the linear regime ($V\rightarrow 0$) the Peltier coefficient (in the above units) coincides with the thermopower coefficient (S) according to the Onsager relation $\Pi/T=S$, and both are given by the solid line. Deviations from the above Onsager relation occur for higher applied voltages (compare the Peltier coefficients depicted by the dashed and dash-dotted curve with the solid curve corresponding to S).

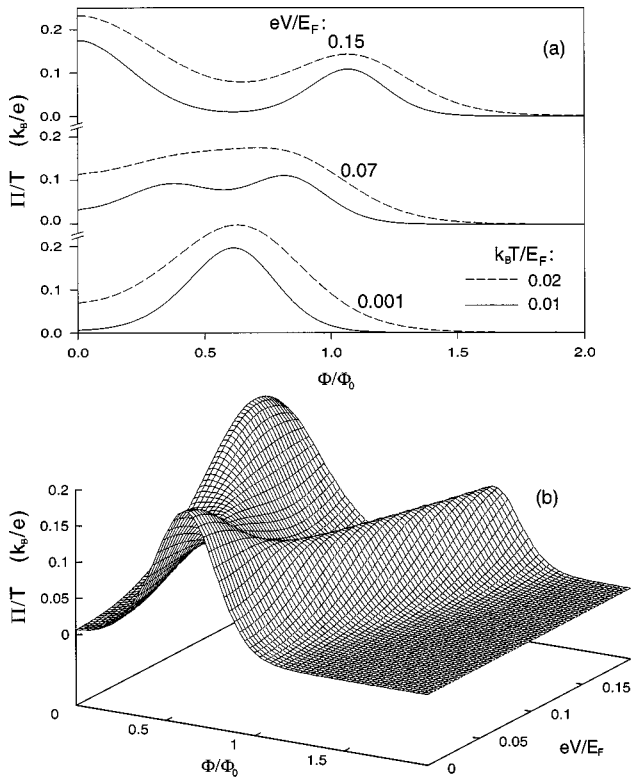

FIG. 2. (a) The Peltier coefficient (Π, in units of k_BT/e) of a 3D wire plotted vs. the dimensionless magnetic flux $\varphi/\varphi_0=H\pi a_0^2e/hc$, with $R/a_0=50$ and $k_Fa_0=4$ (corresponding to three conducting channels for $H=0$ and $V\rightarrow 0$). Different curves correspond to the marked values of the applied voltage (V in units of ε_F/e), and in each case for two different temperatures (T, in units of ε_F/k_B). (b) The Peltier coefficient of the wire plotted vs φ/φ_0 and eV/ε_F, for $k_BT/\varepsilon_F=0.01$.

axis (z) are taken to be circles of radii $a(z)$.[14] In calculations involving a magnetic field it is taken to be parallel to the wire's axis. Assuming that the function $a(z)$ is slowly varying on the scale of k_F^{-1} (k_F is the Fermi wave vector) the electronic transmission probability may be calculated in the adiabatic approximation.[15,16] In this case the transmission probability has a diagonal form (no mode mixing) (Ref. 17)

$$T_{mn;mn}(E)=1+\exp\{-2\pi[E-E_{mn}(0)]/[-(\hbar^2/m^*)\times E''_{mn}(0)]^{1/2}\}, \tag{12}$$

where $E_{mn}(0)$ are the transverse electronic energy levels in the narrowest part of the wire ($z=0$), which we calculate in the hard-wall potential approximation; $E''_{mn}(0)=\partial^2E_{mn}(0)/\partial z^2$, $m=0,\pm 1,...$, and $n=1,2,...$ are the quantum numbers.

We examine first the differential Peltier coefficient of the nanowire, Π [Eq. (11)]. In the absence of a magnetic field the transverse energy levels $E_{mn}^{(o)}$ [see Eq. (12)] are given by the expression $E_{mn}^{(o)}=\hbar^2\gamma_{mn}^2/2m^*a^2(z)$,[16] where γ_{mn} are the zeros of the Bessel function. To calculate the Peltier coefficient we note from Eq. (11) that $\Pi=TG^{-1}(\partial I_s/\partial V)|_{\Delta T=0}$, where $G=(\partial I/\partial V)|_{\Delta T=0}$ is the differential electric conductance. Taking the indicated derivatives of Eqs. (1) and (2) with respect to V and (numerically) evaluating the resulting integrals over the energy, in conjunction with Eq. (12), yields then the value of Π.

The variation of the Peltier coefficient as a function of the dimensionless parameter k_Fa_o is shown in Fig. 1 for $k_BT=0.01\varepsilon_F$, $R/a_o=50$, and several values of the applied voltage V [$R=1/a''(0)$ is the axial radius of curvature that determines the effective length of the wire]. First, we note that the Peltier coefficient has a peaklike structure, with the positions of the peaks as a function of $k_Fa_o[a_o\equiv a(0)]$ determined by the sequence of zeros of the Bessel function γ_{mn} and the magnitude of the applied voltage. These peak positions coincide with the positions of the differential conductance steps calculated at the same values of the applied voltages.[7] The Peltier coefficient for $V\rightarrow 0$ (solid lines in the top and bottom curves in Fig. 1) coincides with the thermopower coefficient[18] (the Seebeck coefficient) S, in accordance with the aforementioned Onsager relation $\Pi=ST$. However, increase of the applied voltage (that is beyond the linear regime) leads to the appearance of new peaks in the Peltier coefficient (dash-dotted line in the top and dashed line in the bottom curves, corresponding to the voltages eV equal to $0.07\varepsilon_F$ and $0.15\varepsilon_F$, respectively), and a consequent violation of the above Onsager relation. Note that the origin of the appearance of the peaks in the Peltier coefficient is that a finite voltage differentiates right- and left-moving electrons leading to the existence of different effective chemical potentials for opposite moving electrons [see Eqs. (1) and (2)]. We recall here that in large classical constrictions,[2] the entropy flow is a linear function of the applied voltage[9] and the Peltier coefficient is a constant (see Sec. II).

In a magnetic field the transverse energy levels of the electrons [$E_{mn}(0)$ in Eq. (12)] are determined by the zeros of the confluent hypergeometric function.[17] The magnetic field shifts the transverse energy levels and removes their m degeneracy,[17,19] resulting in the appearance of an oscillating

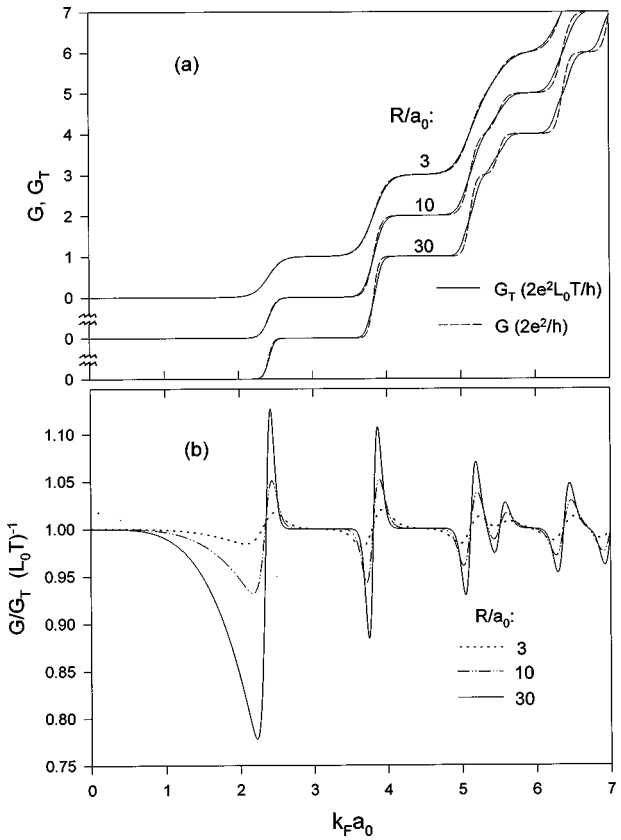

FIG. 3. The electrical conductance (G, in units of $2e^2/h$, denoted by the dashed line) and the thermoconductance (G_T, in units of $2e^2L_0T/h$, denoted by the solid line) in (a) and their ratio in (b) plotted vs the dimensionless parameter k_Fa_0, with $H=0$ and $k_BT/\varepsilon_F=0.01$. The different curves correspond to the three marked values of the parameter R/a_0.

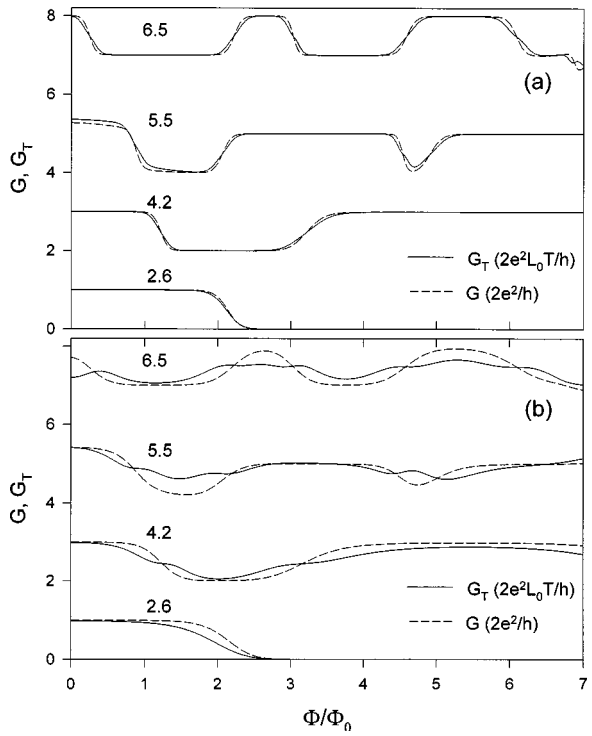

FIG. 4. The conductance (G, in units of $2e^2/h$, denoted by the dashed line) and the thermoconductance (G_T, in units of $2e^2L_0T/h$, denoted by the solid line) of a 3D wire vs the dimensionless magnetic flux φ/φ_0, with $R/a_0=100$ and $k_BT/\varepsilon_F=0.004$ in (a) and $k_BT/\varepsilon_F=0.02$ in (b). Different curves correspond to the marked values of k_Fa_0.

structure of the Peltier coefficient similar to oscillations of the thermopower coefficient discussed by us earlier.[18] In Fig. 2(a) we display, for several values of V and the temperature T, the dependence of the Peltier coefficient on the dimensionless magnetic flux φ/φ_0 ($\varphi=\pi a_0^2H$ is the magnetic flux through the narrowest part of the wire and $\varphi_o=hc/e$ is the flux quantum) for a wire with $R/a_0=50$ and $k_Fa_0=4$ corresponding to three conducting channels at $H=0$ and $V\to0$. At $V\to0$, the magnetic field dependencies of the Peltier and thermopower coefficients are the same (bottom curve). Increase of the voltage leads to differences in the behavior of the Peltier (upper curves) and thermopower coefficients. The behavior of the Peltier coefficient can be influenced either by an applied magnetic field, an applied voltage or combinations of the two as shown in Fig. 2(b) for $k_BT=0.01\varepsilon_F$.

Next we examine the thermoconductance [Eq. (6)] in quantum nanowires.[20] As noted above [see Eq. (7) and related discussion] in a classical constriction the thermal (G_T) and electric (G) conductances obey the Wiedemann-Franz law. However, in quantum wires the Wiedemann-Franz law is violated, due mainly to the strong energy dependence of the transmission probabilities [Eq. (12)] near ε_F.[21] To illustrate this we plot the electric conductance (G, dashed line, in units $2e^2/h$) and the thermoconductance (G_T, solid line, in units $2e^2L_oT/h$) in Fig. 3(a), and their ratio [in Fig. 3(b)], versus k_Fa_o for $k_BT=0.01\varepsilon_F$ and for different values of the dimensionless parameter $[a_0a''(0)]^{-1}=R/a_0$. Note that smearing of the steps due to tunneling effects in the shorter wires restores the Wiedemann-Franz behavior. Deviations from the Wiedemann-Franz law are reduced also at low temperatures because of the decrease of the energy region in the electrons distribution [that is, sharper Fermi functions in Eqs. (1) and (2)] contributing to the transport coefficients.[3,4]

The thermoconductance of the wire may be also affected by applied magnetic fields. In Fig. 4 we display the magnetic field dependence of the electrical and thermal conductances for (a) $k_BT=0.004\varepsilon_F$ and (b) $k_BT=0.02\varepsilon_F$ for $R/a_0=100$, and for different values of the parameter k_Fa_0($k_Fa_0=2.6$, 4.2, 5.5, and 6.5) corresponding at $H=0$ to 1, 3, 5, and 8 conducting channels, respectively. Such a behavior of the transport coefficients demonstrates, both for the electrical and thermal transport, a ''magnetic switch'' effect and even magnetic blockade (in wires with small values of k_Fa_0). At lower temperatures the dependence of G and G_T on the magnetic field are increasingly similar to each other [compare Figs. 4(a) and 4(b)].

IV. SUMMARY

The analysis presented above shows that studies of thermal transport in nanowires can be used as independent measurements, in addition to those of the electric current, for investigations of the properties of three-dimensional nanostructures. An important conclusion is that the thermal transport as well as the electric one,[7,17] can be controlled by external parameters, such as an applied voltage and/or a magnetic field. Such control is of particular importance for

investigations of (free-standing) nanowires, where the applications of modern experimental techniques for generation of such wires [1(c)] (based on scanning tunneling and force microscopy, mechanical break junctions, and pin-plate methods) do not allow full mechanical control and reproducibility from one experiment to the other.

We have demonstrated here theoretically a nonlinear Peltier effect in 3D nanowires, exhibited by the appearance of peaks at finite voltages compared to the linear-response regime (deviation from the Onsager relation, Fig. 1), as well as magnetic field induced oscillations of the Peltier coefficient (Fig. 2). In addition we have investigated the thermoconductance of nanowires in a magnetic field, including magnetic blockade of the thermal transport (Figs. 3 and 4). Such a behavior of the thermal transport coefficients in nanowires is due to the influence of the external fields on the spectrum of electronic states in the nanoconstrictions, allowing one to change and control the number of conducting channels. These effects might be experimentally observed in magnetic fields with fluxes of the order of the flux quantum (see detailed discussion in Ref. 17), and voltages, such that eV is of the order of the spacing between the electronic energy levels. Such conditions, which might be difficult to achieve for typical metals, can be readily obtained for semimetallic wires even in the linear voltage regime. Furthermore, the high sensitivity of the thermal transport to the applied voltage may allow observation of the phenomena discussed above in the nonlinear regime, even for typical metals (see also discussion in Ref. 7).

ACKNOWLEDGMENTS

This research was supported by the U.S. Department of Energy, Grant No. FG05-86ER45234. Calculations were performed at the Georgia Tech. Center for Computational Materials Science.

[1] (a) A. M. Duif, A. G. M. Jansen, and P. Wyder, J. Phys.: Condens. Matter **1**, 3157 (1989); (b) C. W. J. Beenakker and H. van Houten, in *Solid State Physics*, edited by H. Ehrenreich and D. Turnbull (Academic, San Diego, 1991), Vol. 44, p. 1; (c) *Nanowires*, edited by P. A. Serena and N. Garcia (Kluwer, Dordrecht, 1997); (d) for a discussion on thermopower and magnetoconductance in three-dimensional quantum nanowires see the article by E. N. Bogachek, A. G. Scherbakov, and U. Landman, *ibid.*, p. 35.

[2] Yu. V. Sharvin, Zh. Eskp. Teor. Fiz. **48**, 984 (1965) [Sov. Phys. JETP **21**, 655 (1965)].

[3] C. R. Proetto, Solid State Commun. **80**, 909 (1991).

[4] H. van Houten, L. W. Molenkamp, C. W. J. Beenakker, and C. T. Foxon, Semicond. Sci. Technol. **7**, B215 (1992).

[5] L. I. Glazman and A. V. Khaetskii, Pis'ma Zh. Eksp. Teor. Fiz. **48**, 546 (1988) [JETP Lett. **48**, 591 (1988)].

[6] J. I. Pascual, J. A. Torres, and J. J. Saenz, Phys. Rev. B **55**, R16 029 (1997).

[7] E. N. Bogachek, A. G. Scherbakov, and U. Landman, Phys. Rev. B **56**, 14 917 (1997).

[8] E. N. Bogachek, A. G. Scherbakov, and U. Landman, Solid State Commun. **108**, 851 (1998).

[9] E. N. Bogachek, I. O. Kulik, and A. G. Shkorbatov, Fiz. Nizk. Temp. **11**, 1189 (1985) [Sov. J. Low Temp. Phys. **11**, 656 (1985)].

[10] U. Sivan and Y. Imry, Phys. Rev. B **33**, 551 (1986).

[11] R. Landauer, Philos. Mag. **21**, 863 (1970).

[12] We restrict ourself here to consideration of the electronic contributions to the entropy and heat flows which are dominant in conductors. Different aspects of classical and quantum heat transport through constrictions originating from phonons were discussed in E. N. Bogachek and A. G. Shkorbatov, Fiz. Nizk. Temp. **11**, 643, (1985) [Sov. J. Low Temp. Phys. **11**, 353 (1985)]; A. G. Shkorbatov, A. Feher, and P. Stefanyi, Physica B **218**, 242 (1996); L. G. C. Rego and G. Kirczenow, Phys. Rev. Lett. **81**, 232 (1998); M. P. Blencowe, Phys. Rev. B **59**, 4992 (1999).

[13] J. M. Ziman, *Principles of the Theory of Solids* (Cambridge University Press, Cambridge, 1986), Chap. 7.

[14] Effects of the cross-sectional shape of 3D quantum nanowires on the electric conductance have been discussed in E. N. Bogachek, A. G. Scherbakov, and U. Landman, Phys. Rev. B **56**, 1065 (1997). In that study it has been shown that deviations from circular symmetry (e.g., elliptical cross-sections) can affect the positions and degeneracies of the transverse energy levels (conducting channels), with a consequent effect on the step structure of the quantized electric conductance; for classical point contacts area preserving changes of the cross-sectional shapes affect the conductance values through the Weyl corrections to the Sharvin (Ref. 2) conductance formula [see discussion following Eq. (5)] which depends only on the cross-sectional area. Consequently, such shape-effects may modify only the positions and heights of the steps in the quantized electronic and thermal conductances and similarly the peak positions of the Peltier coefficients, but otherwise they do not change the trends and conclusions discussed in this paper.

[15] L. I. Glazman, G. B. Lesovik, D. E. Khmel'nitskii, and R. I. Shekhter, Pis'ma Zh. Eksp. Teor. Fiz. **48**, 218 (1988) [JETP Lett. **48**, 238 (1988)].

[16] E. N. Bogachek, A. M. Zagoskin, and I. O. Kulik, Fiz. Nizk. Temp. **16**, 1404 (1990) [Sov. J. Low Temp. Phys. **16**, 796 (1990)].

[17] E. N. Bogachek, A. G. Scherbakov, and U. Landman, Phys. Rev. B **53**, R13 246 (1996).

[18] E. N. Bogachek, A. G. Scherbakov, and U. Landman, Phys. Rev. B **54**, R11 094 (1997).

[19] E. N. Bogachek, M. Jonson, R. I. Shekhter, and T. Swahn, Phys. Rev. B **47**, 16 635 (1993); **50**, 18 341 (1994).

[20] From the definition in Eq. (6), G_T is given by the derivative of the heat current ($Q=TI_s$) with respect to ΔT under the condition of vanishing electric current ($I=0$). Evaluation of G_T proceeds by first solving Eq. (1) for V with $I=0$ and $T_2-T_1=\Delta T$, and then using this value in subsequent calculation of the integrals in the expression for the derivative of I_s [see Eq. (2)] with respect to ΔT, in conjunction with the transmission probabilities [Eq. (12)].

[21] Deviations from the Wiedemann-Franz law in two-dimensional semiconducting constrictions were discussed in Refs. 3 and 4.